



Western Michigan University
ScholarWorks at WMU

Honors Theses

Lee Honors College

4-21-2023

Characterization of *Shinella* 6-hydroxy-(L)-nicotine oxidase (6HLNO-SE)

Kaitrin Funckes
Western Michigan University

Follow this and additional works at: https://scholarworks.wmich.edu/honors_theses

 Part of the Chemistry Commons

Recommended Citation

Funckes, Kaitrin, "Characterization of *Shinella* 6-hydroxy-(L)-nicotine oxidase (6HLNO-SE)" (2023). *Honors Theses*. 3738.

https://scholarworks.wmich.edu/honors_theses/3738

This Honors Thesis-Open Access is brought to you for free and open access by the Lee Honors College at ScholarWorks at WMU. It has been accepted for inclusion in Honors Theses by an authorized administrator of ScholarWorks at WMU. For more information, please contact wmu-scholarworks@wmich.edu.



Characterization of *Shinella* 6-hydroxy-(L)-nicotine oxidase (6HLNO-SE)

Kaitrin Funckes

Table of Contents

<i>Abstract</i>	3
<i>Introduction</i>	4
<i>Methods</i>	10
<i>Results</i>	14
<i>Discussion</i>	23
<i>References</i>	26
<i>Contributions & Acknowledgements</i>	27

Abstract

6-hydroxy-(L)-nicotine oxidase, isolated from the organism *Shinella* sp. HZN7 (6HLNO-SE), is an enzyme that during the catabolism of nicotine catalyzes the oxidation of (S)-6-hydroxynicotine to 6-hydroxypseudooxynicotine. This enzyme is a member of the monoamine oxidase (MAO) structural family of flavoproteins, which contain a highly conserved FAD-binding domain. Within the binding domain is a conserved lysine residue that can be traced throughout evolutionary history in this family. 6HLNO isolated from *Arthrobacter nicotinovorans* serves as a model enzyme for the one isolated from *Shinella* as both catalyze the same reaction in this biochemical pathway and much has been studied about the *Arthrobacter* enzyme. However, the lysine residue in *Shinella* does not reside in the same location as it has throughout evolutionary history and these two enzymes share little common amino acid identity. This study aims to understand the mechanism of 6HLNO-SE as compared to that of *Arthrobacter* by using steady-state and transient kinetic assays via an O₂ probe and stopped-flow experimentation to analyze mutagenesis effects and pH-dependence of the active site residues. Results demonstrate that the lysine residue as conserved throughout evolutionary history is critical for reactivity in 6HLNO-SE and that, though distantly related, the *Shinella* and *Arthrobacter* enzymes have very similar behavior.

Introduction

In recent years nicotine has grown to be of large concern for communities globally. There are many impacts nicotine use has on human health and on the environment. Tobacco use contributes to the largest source of preventable cancers, while nicotine itself has high carcinogenic potential. Nicotine is one of the most toxic and addictive poisons known. It targets the peripheral and central nervous systems and has been shown to change the way synapses in the brain are formed which are involved with attention and learning¹. This becomes especially concerning when it is considered how much more likely young individuals are to use nicotine products in the form of e-cigarettes, not to mention the other health risks involved in the use of these products². Production of tobacco has one of the largest impacts on the environment worldwide, with an estimation of 211,000 hectares of deforestation annually and one of the largest contributors to greenhouse emissions³. Globally, tobacco use accounts for 5.4 billion deaths per year and it is estimated that 1 billion individuals could die in this century if current tobacco use does not change¹. While the WHO has implemented an international treaty to reduce the production, promotion, and sales of tobacco products and is making steady progress in control of tobacco use worldwide¹, it can be seen that swift action in the nicotine epidemic is needed.

6-hydroxy-(L)-nicotine oxidase, isolated from the organism *Shinella* sp. HZN7, is a member of the structural family of monoamine oxidase flavoproteins (MAO). This enzyme catalyzes the oxidation of (S)-6-hydroxynicotine to 6-hydroxypseudooxynicotine⁴. Another enzyme, 6HLNO isolated from *Arthrobacter nicotinovorans* catalyzes the same reaction and is a member of this family of enzymes. The MAO family contain a conserved FAD-binding domain and can be found amongst its members. Another enzyme belonging to this family, nicotine

oxidoreductase (NicA2), isolated from *Pseudomonas putida* S16, catalyzes the degradation of nicotine and serves as a potential therapeutic for nicotine addiction⁵. NicA2 has a sequence that is 30% identical to that of LHNO isolated from *Arthrobacter*, demonstrating that it is indeed a flavoprotein oxidase and belongs to the MAO family⁶ (**Figure 1**). However, recent research on NicA2 suggests that the enzyme reacts inappreciably with molecular oxygen as its terminal electron acceptor, a common characteristic of MAO family enzymes (although not all follow this pattern, as is the case with NicA2). It has recently been identified as a dehydrogenase with the natural electron acceptor of NicA2 being a cytochrome c (CycN) specific to *Pseudomonas putida* S16⁵. Typical flavoproteins can be observed in two catalytic cycles: a reductive half-reaction and an oxidative half-reaction. In the reductive half-reaction, the oxidized FAD is reduced by the substrate to produce FADH₂, a reduced FAD. In the oxidative half-reaction, the FAD is oxidized from FADH₂ back to FAD by reacting with O₂ (the reaction NicA2 is unable to perform at an appreciable rate)⁵ or other oxidants (**Figure 2**). In the case of *Arthrobacter* and *Shinella*, both react rapidly with molecular oxygen⁶. During their catalytic cycles, the enzymes will react with their substrate, 6-hydroxy-nicotine (6OHN), to reduce the flavin, while O₂ will oxidize it and return the enzyme to its original state, as determined by previous studies^{4,6}.

Phylogenetic tree of the MAO structural family

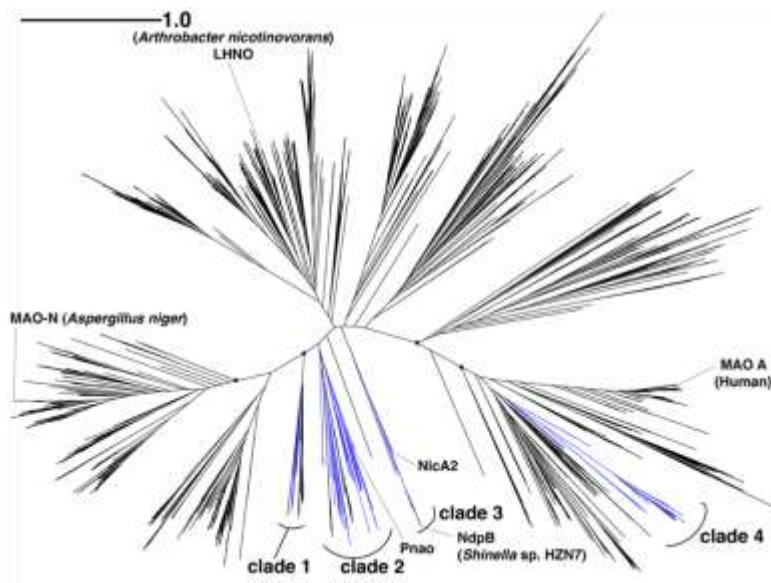


Figure 17: A phylogenetic tree of the MAO structural family of proteins.

Flavin-Dependent Redox Reaction

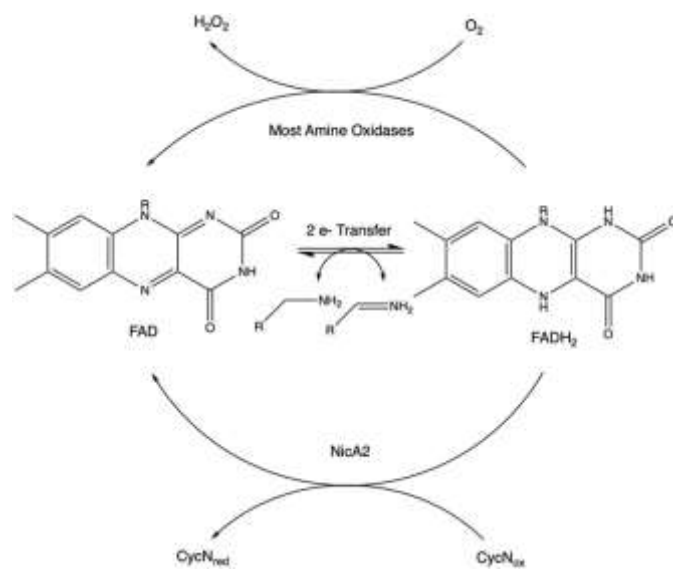


Figure 2: A scheme showing the redox reaction catalyzed by most flavin-dependent enzymes as well as NicA2. The reaction catalyzed by NicA2 is represented on the bottom while most other amine oxidases is represented by the arrow at the top of the scheme. This is the reaction seen for both *Arthrobacter* and *Shinella* 6HLNO enzymes.

Within the conserved flavin domain in the MAO structural family is a conserved lysine residue in the active site adjacent to the flavin's isoalloxazine, which has been shown to be critical to the rapid reaction of these enzymes with molecular oxygen⁴ (**Figure 3**). Curiously, this lysine residue is present in NicA2, yet the enzyme reacts poorly with molecular oxygen. However, this critically conserved lysine residue, while present in *Arthrobacter* 6HLNO, is *absent* in *Shinella* 6HLNO (6HLNO-SE), at least at the canonical position within the sequence of this enzyme family. These enzymes belong to the same MAO structural family as NicA2, and both catalyze the same reaction: the oxidation of (S)-6-hydroxynicotine to 6-hydroxypseudooxynicotine⁴. While sharing the ability to catalyze the same reaction, these enzymes also have little common amino acid identity, making their evolutionary relationship distant from one another (**Figure 1**). 6HLNO-SE has a glutamate residue (Glu292 in 6HLNO-SE) at the amino acid position where the conserved lysine is normally found. The structure of 6HLNO-SE revealed that a lysine residue at another amino acid position (Lys331 in 6HLNO-SE), which is not present in most MAO enzymes, has its side chain located in a very similar location as that of the highly conserved lysine in other MAO enzymes (**Figure 4**). Since 6HLNO-SE has been shown to react rapidly with molecular oxygen, it was hypothesized that this new Lys331 may be playing the same role as the highly conserved lysine in other MAOs towards promoting the rapid reaction of FADH₂ with molecular oxygen. Much is understood now about the mechanism and structure of *Arthrobacter* 6HLNO⁴. And while structural detail of 6HLNO from *Shinella* is known, its mechanism of action remains to be understood in depth. The important active site residues in *Arthrobacter* have been characterized by mutagenesis and pH

effects to understand their specificity and contributions to enzymatic activity. Results demonstrate the significance of the conserved lysine residue to reactivity⁴. The purpose of this study is to mimic previous studies done on the *Arthrobacter* 6HLNO with that of *Shinella* 6HLNO (6HLNO-SE), and to probe the importance of Glu292 and Lys331 on the enzyme's activity. It is hypothesized that though these enzymes have distant evolutionary relation, they will demonstrate similar activity based on the relative structures of their active sites and that the lysine residue identified in 6HLNO-SE will be determined to be critical for reactivity. While 6HLNO itself does not react with nicotine, it catalyzes a critical step in the mechanism and it is hopeful that by understanding more about this enzyme, more can be discerned about NicA2 and aid in the search for a therapeutic to overcome nicotine addiction.

A scheme of the reaction catalyzed by LHNO

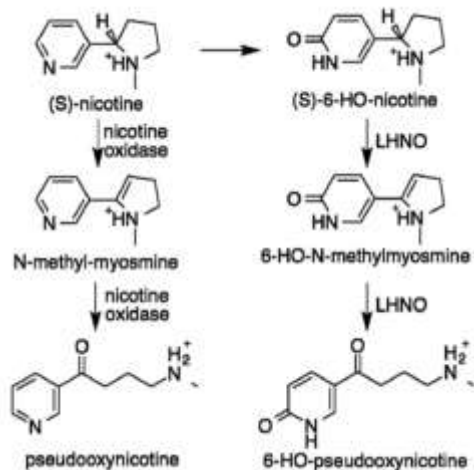


Figure 3⁶: A scheme demonstrating the conversion of (S)-6-hydroxynicotine to 6-hydroxypseudooxynicotine as catalyzed by LHNO. This can be seen in the right-hand side of the figure where LHNO is involved in the catalysis of (S)-6-hydroxynicotine to 6-hydroxy-methylmyosmine and then to 6-hydroxypseudooxynicotine⁶.

Active Sites of *Arthrobacter* and *Shinella* 6HLNO Enzymes

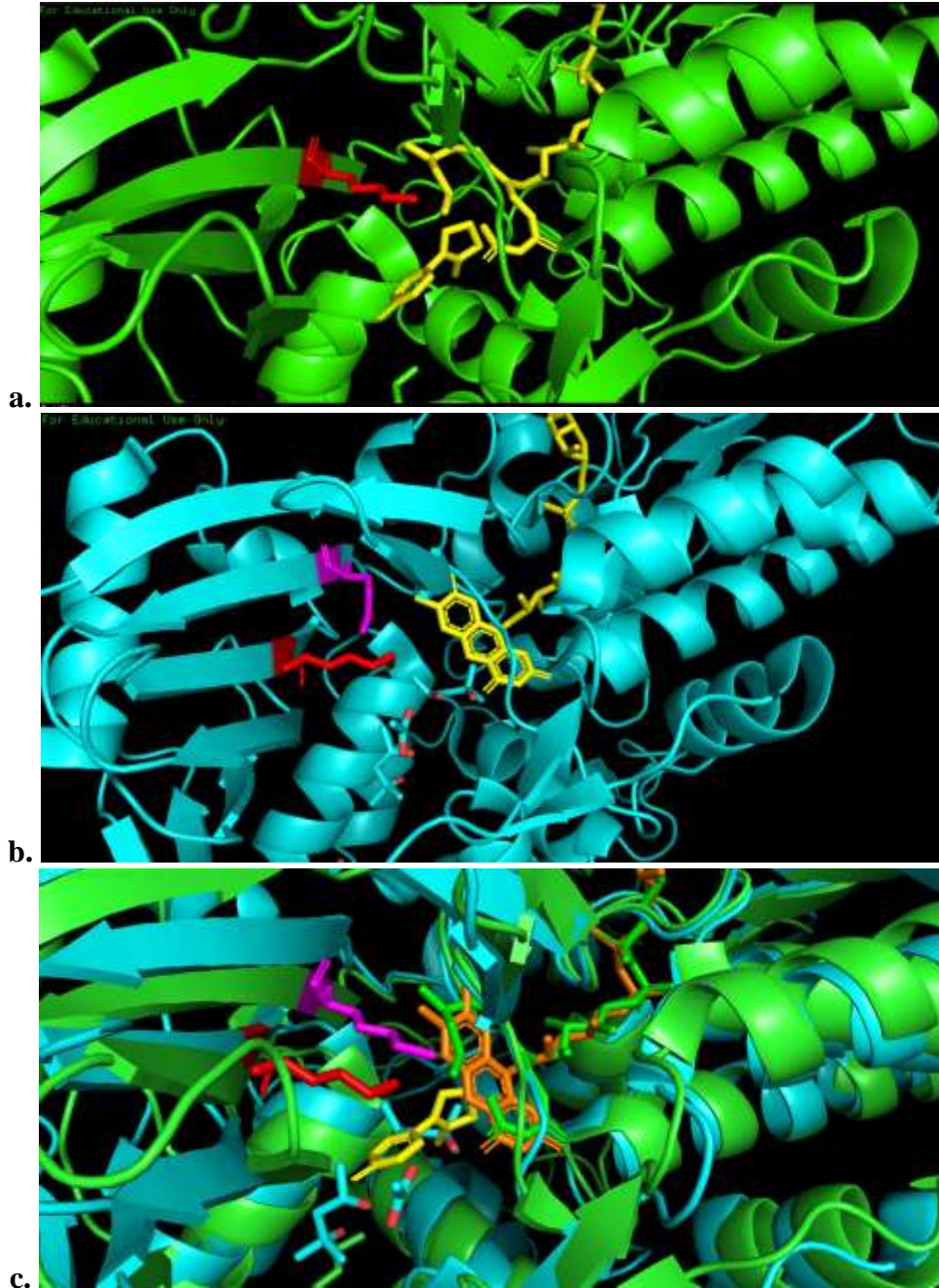


Figure 4: This figure shows the active sites of *Arthrobacter* and *Shinella* 6HLNO enzymes. The critical lysine residue in *Arthrobacter* (a), is highlighted in red while the flavin is highlighted in yellow. The critical lysine residue in *Shinella* (b) is also highlighted in red as well as the flavin colored in yellow. Also shown is the glutamate residue, highlighted in magenta. The active sites are shown superimposed on one another (c) where the *Shinella* lysine is highlighted in red and the flavin in orange, while the enzyme itself is cyan. The *Arthrobacter* lysine is highlighted in magenta while the flavin is highlighted in yellow and the enzyme itself is green. The superimposed image demonstrates the location between the critical lysine residues between the enzymes.

Methods

Strain and culture conditions

The plasmid for *Shinella* 6-hydroxy-(L)-nicotine oxidase was obtained from Twist Biosciences as a synthesized construct with a C terminal histidine tag. General growth of strains was performed in lysogeny broth (LB) medium and antibiotic selection included 100 $\mu\text{g mL}^{-1}$ of kanamycin (Kan) for each 6HLNO-SE plasmid. Selection plates used the same formula as the liquid media but instead used 40 g L^{-1} Luria agar (Research Products International, RPI). The protein expression media was 12 g L^{-1} tryptone, 24 g L^{-1} yeast extract, 50.4 g L^{-1} glycerol, 2.13 g L^{-1} K_2HPO_4 , and 12.54 g L^{-1} KH_2PO_4 . The cells used for protein expression were *E. coli* BL21 (DE3).

Purification for steady-state and stopped-flow assays

6HLNO-SE mutants were amplified via PCR (Applied Biosystems Veriti 96 well Thermal Cycler) using the primers in **Table 1**. Mutations were observed via a diagnostic agarose gel. Then the PCR reactions were DpnI digested for 30 minutes before transformation into *E. coli* DH5 α cells. These samples were miniprep (Zymo Research Plasmid Miniprep – Classic) and sequences verified via Sanger sequencing. Then, the plasmids were transformed into *E. coli* BL21 (DE3) for expression overnight on LB/Kan plates at 37°C. Then, colonies were chosen for growth in 100 mL LB/Kan media overnight before dilution into protein expression media. This was grown to an OD₆₀₀ of ~0.6 and then transferred to 20°C shaker and induced with 200 μM IPTG overnight. Cells were spun down the next day and the pellet stored at -20°C until purification. A lysis buffer of 50 mM sodium phosphate, 300 mM NaCl, 20 mM imidazole, and 10% glycerol was used to resuspend the cell pellet, to which protease inhibitor and benzonase

nuclease was added. This was sonicated on ice for 5 minutes and then spun down at 19,000 RPM and 4°C for 20 minutes. The supernatant was run over a column containing 5 mL of Ni-NTA resin pre-equilibrated with lysis buffer. A buffer containing 50 mM sodium phosphate, 300 mM NaCl, 250 mM imidazole, and 10% glycerol was used to elute the protein. The protein elution was then further purified using size exclusion chromatography by fast protein liquid chromatography (FPLC) using a buffer containing 40 mM HEPES, 100 mM NaCl, and 10% glycerol at a pH of 7.5. The purified protein fractions were concentrated and flash-frozen using liquid nitrogen and then stored at -80°C until usage. By using the absorbance of the bound FAD cofactor having an extinction coefficient at 450 nm of $\epsilon = 11,300 \text{ M}^{-1} \text{ cm}^{-1}$, the concentration of 6HLNO-SE was determined.

Steady-state kinetic assays

The reaction of 6HLNO-SE with 6-hydroxy-nicotine (6OHN) was monitored by use of an oxygen electrode (Hansatech Instruments Oxygraph System Plus). This was done to monitor the effects of the mutations made and monitor the pH dependence of kinetic parameters. Reactions concerning the mutants were performed in 40 mM HEPES, 100 mM NaCl, 10% glycerol, pH = 7.5, at 4°C. The pH-dependent reactions were performed in a range from 5.5-10.0 at 4°C. Buffers were prepared at room temperature and assays performed at 4°C. The buffers used were 40 mM CAPS, 40 mM CHES, and 40 mM MES. Each contained 100 mM NaCl and 10% glycerol. The reaction volume was 1 mL, containing various concentrations of 6OHN, and 6HLNO-SE at concentrations between 20 nM-2 μM . Higher concentrations were needed for some mutants and pH values in order to detect enzyme activity.

By use of KaleidaGraph, the linear portion of the reaction was used to determine the velocity of the reaction. The initial velocity of reaction was divided by the enzyme concentration used for each reaction. The steady-state kinetic parameters were determined by taking these values and fitting them to the Michaelis-Menten equation. For the pH-dependent assays, the pH was then graphed against the log of k_{cat} , s^{-1} where a normal distribution of the enzyme activity relative to pH value was obtained. The pK_a values were determined based on equation 1 below, where c is the maximum reaction rate. The substrate, 6OHN, is a racemic mixture. So, this was corrected for in kinetic analysis to be the concentration of the desired L stereoisomer (6-hydroxy-(L)-nicotine), by dividing the concentration in half due to the proportion of L to R stereoisomers.

$$\log k_{cat} = \log \frac{c}{1 + \frac{10^{-pH}}{10^{-pK_{a1}}} + \frac{10^{-pK_{a2}}}{10^{-pH}}} \quad (1)$$

Stopped-flow assays

Stopped-flow experiments were each performed in 40 mM HEPES, 100 mM NaCl, 10% glycerol, pH = 7.5, at 4°C. The instrument implemented was a TgK Scientific SF-61DX2 KinetAsyst stopped-flow instrument. Each experiment was performed anaerobically by placing 35 μ M 6HLNO-SE and mutations in a glass tonometer and cycling between argon and vacuum⁸. In the experiments performed to monitor the reaction with O₂, 6HLNO-SE was titrated with 20 mM 6-hydroxy-nicotine oxidase (6OHN) using a gas tight syringe until the reduced flavin was visible in the absorbance spectrum. For O₂-dependent reactions, the tonometer was placed on the machine and mixed with buffer containing different O₂ concentrations, which were prepared by using a gas blender at various N₂/O₂ ratios. These reactions were monitored using the stopped-flow's CCD detector. For the 6OHN-dependent reactions, anaerobic 6OHN (made so by

sparging with argon) was prepared at various concentrations in buffer, and the reaction was monitored at 450 nm using the instrument's single wavelength PMT detector.

Data was analyzed using KaleidaGraph. Traces for the reactions with O₂ at 450 nm were fit to equation 2, a single exponential function, to obtain the observed rate constant value (k_{obs}) for each different O₂ concentration. For reactions with 6OHN, the traces were fit to a sum of exponentials, given by equation 3, for obtaining the observed rate constant for the two kinetic phases in these reactions. In the given equations, ΔA the amplitude for the phase is given by ΔA , the first order rate constant is given by k_{obs} , and the absorbance at the end of the reaction is given by A_{∞} . As before, the racemic mixture of 6OHN was corrected for in kinetic analysis to be the concentration of the desired stereoisomer.

$$y = \Delta A e^{-k_{obs}t} + A_{\infty} \quad (2)$$

$$y = \Delta A_1 e^{-k_{obs}t} + \Delta A_2 e^{-k_{obs}t} + A_{\infty} \quad (3)$$

<i>Primer Name</i>	<i>Primer Sequence (5' to 3')</i>
K331M Forward	CATTTTAATGATTACCATCGGACGTCAGAGC
K331M Reverse	GTAATCATTAAAATGGTACCCAATTCATCATCA
K331S Forward	CATTTTAAGTATTACCATCGGACGTCAGAGC
K331S Reverse	GTAATACTTAAAATGGTACCCAATTCATCATCA
E292K Forward	CGGAGCCAAATTATACGTACATGTACGTCAGAACC
E292K Reverse	TATAATTTGGCTCCGTCAGCCATTTC
E292T Forward	CGGAGCCACATTATACGTACATGTACGTCAGAACC
E292T Reverse	TATAATGTGGCTCCGTCAGCCATTTC

Table 1: Primers used in this study.

Results

Selection of Active Site Residues

Residues were chosen based on the comparison between active sites of 6HLNO from that of *Shinella* as compared to *Arthrobacter*. The *Arthrobacter* lysine residue at position 287 (**Figure 4a**) has been shown to have the greatest impairment on reactivity by mutagenesis assays⁴, which makes this residue of highest interest. The lysine residue was demonstrated to serve an important role in both reductive and oxidative reactions. Due to its position within the flavin domain, it is able to establish the reactivity between both substrates of oxygen as well as (S)-6-hydroxynicotine⁴. The *Shinella* active site also contains a lysine residue (**Figure 4b**) which is hypothesized to be critical to activity in oxidative and reductive reactions; however, it is shifted from the location observed in *Arthrobacter* (**Figure 4c**), residing at position 331. The residues predicted to have the greatest significance to reactivity as well as to demonstrate comparable activity between the enzymes were K331 and E292. The significance of these residues rises from their relative location in the active site of *Shinella* 6HLNO compared to *Arthrobacter* 6HLNO and NicA2. NicA2 has a lysine residue and a serine residue, respectively, at the positions corresponding to E292 and K331 in 6HLNO-SE. Therefore, a E292K/K331S double mutant of 6HLNO-SE was also generated to determine if NicA2's lysine architecture leads to a functional variant of 6HLNO-SE that still reacts rapidly with molecular oxygen. The mutations selected are given in **Table 3** below.

Mutations to 6HLNO-SE Active Site Residues

K331M
E292T
E292K + K331S

Table 2: Mutations made to the *Shinella* 6HLNO enzyme in the active site.

The residue predicted to have the greatest impairment on activity is the lysine at position 331. By mutating to a methionine, the positive charge is eliminated and thus should disrupt activity. The next position focused on was glutamate at position 292. As seen in the active site (**Figure 4b**), the lysine and glutamate residues are in close proximity to one another. By interaction of opposing charges, a salt bridge is proposed to be formed. Therefore, the glutamate was mutated to a threonine to disrupt this interaction. Threonine was chosen to replace this glutamate because the ancestral protein that existed prior to the emergence of the lineage containing 6HLNO-SE likely contained a threonine at this position⁴. The last mutation is a double mutant based on the active site of NicA2. In this enzyme, there is a lysine at position 292 and a serine at 331.

Mutagenesis Steady-State Assays

Steady-state kinetic assays were performed with the oxygen electrode to monitor the reactivity of the mutants of 6HLNO-SE, as well as wild type 6HLNO-SE to serve as a benchmark. The enzyme turnover number and Michealis-Menton constant results are shown below in **Table 3**. Both sets of values recorded are apparent values since reactions were performed at low concentrations of oxygen. As predicted, the lysine residue caused the largest disruption in enzymatic activity, displaying the smallest turnover number; compared to wild-

type, the turnover number for this mutant was about 430 times smaller. The K_M for this mutant displays a value about half that of wild type. The E292T mutation also caused a disruption in activity, yielding the second largest impairment to the enzyme, with a k_{cat} value about 260 times smaller than wild-type, while the K_M value is about 100-fold smaller than wild type. This suggests that the salt bridge between the lysine and glutamate residues in the active site of the enzyme are important for reactivity with O_2 . The last mutation, E292K + K331S, which was meant to insert NicA2's lysine architecture into *Shinella* 6HLNO, gave an intriguing result. The mutant enzyme still had considerable activity, only about 10-fold lower than wild type. The K_M observed for this mutant is about 10-fold smaller than wild type. Overall, the lysine to methionine mutation impacted enzyme activity the greatest, demonstrating the significance of this residue in fully catalyzing this reaction in the presence of molecular oxygen.

Enzyme Turnover

	$k_{cat, \text{ apparent}}, s^{-1}$	$K_M, \text{ apparent}, \mu\text{M}$
Wild type	42.202 ± 1.255	28.3 ± 4.616
K331M	0.09883 ± 0.005	10.083 ± 4.505
E292T	0.16404 ± 0.004	ND
E292K + K331S	3.0927 ± 0.112	6.3367 ± 2.914

Table 3: Enzyme turnover number and Michelis-Menton constant for each mutation and wild-type 6HLNO-SE. This is the apparent k_{cat} value because the concentration of O_2 is low.

ND: The value for this mutant could not be determined based on the kinetic plot.

pH-Dependent Steady-State Assays

The oxygen electrode was utilized to perform pH-dependent steady-state kinetic assays to monitor the effects of pH on enzyme activity. The pH range over which enzyme activity with 6-hydroxy-nicotine oxidase (6OHN) was determined was 5.5-10. Outside this range the enzyme lost activity, and therefore could not give reliable results. As shown in **Figure 5a** below, the enzyme activity decreases in the pH range of 5.5-6 and on the lower end and a similar observation is seen in the range of 9.5-10 on the upper end. The data was fit and analyzed to obtain pK_a values for the active site of the enzyme; these results are shown in **Table 4** below. The pK_1 value of 6.6 is the acidic value and pK_2 of 9.2 the basic. The wild type *Arthrobacter* 6HLNO enzyme shows a pK_1 of 7.0 and a pK_2 of 10.6⁴. The acidic pK_a is for 6HLNO-SE is only slightly lower than that of the *Arthrobacter* enzyme whereas the basic pK_a is about 1.4 units lower. The basic pK_a of 10.6 in *Arthrobacter* was assigned to the highly conserved lysine residue⁴; the considerably lower basic pK_a observed in the *Shinella* enzyme here may therefore be due to the lysine at the alternative position in this enzyme, which may have a different electrostatic environment than the highly conserved one in the *Arthrobacter* enzyme. The acidic pK_a in *Arthrobacter* has been connected with the enzyme-bound substrate in its ability to take multiple conformations in either protonated or deprotonated states⁴. Since it is observed that the *Shinella* enzyme a very similar acidic pK_a value, it could be assumed that the same is true of 6HLNO-SE. Both enzymes are observed to give a bell-shaped profile (**Figure 5**), demonstrating their similar behavior and activity. This suggests that while these enzymes have distant relation, they still are able to perform in a similar manner catalyzing the oxidation of (S)-6-hydroxynicotine to 6-hydroxypseudooxynicotine.

pH profile for *Shinella* and *Arthrobacter* 6HLNO

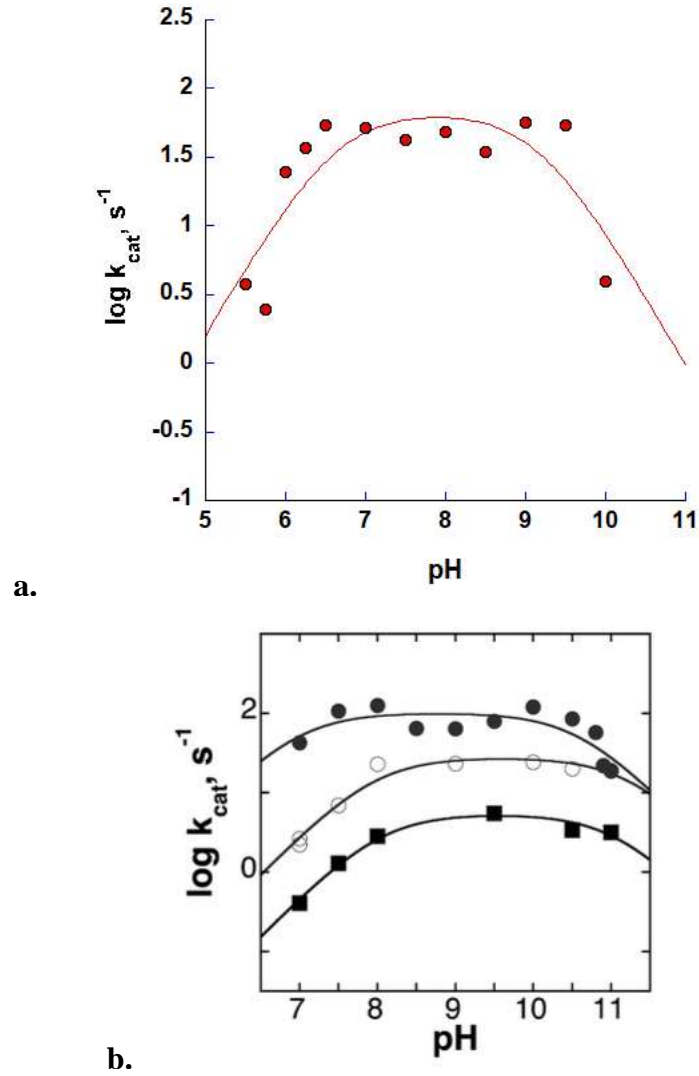


Figure 5: pH profile for wild type 6HLNO-SE (a). This figure shows the pH against the log of k_{cat} . The pH profile for *Arthrobacter* 6HLNO (b⁴) is also shown. Wild type is shown by the closed circles.

pK_a values for 6HLNO-SE

pK_1	pK_2
6.621	9.163

Table 4: This table shows the pK_a values for 6HLNO-SE based on the fit of the pH profile. pK₁ references the acidic pK_a value of the enzyme and pK₂ references the basic pK_a value of the enzyme.

Stopped-Flow Assays

Stopped-flow assays were employed to fully understand how mutagenesis impacted enzymatic activity. Due to the presence of a flavin cofactor in the active site of the enzyme, these reactions can be monitored via absorbance changes. In one condition, the enzyme was reacted with the substrate 6-hydroxy-nicotine (6OHN) for the flavin to reach its reduced form in the absence of oxygen (**Figure 6** and **Table 5**). In the other condition, the flavin was reduced with 6OHN and then reacted with molecular oxygen to reach its oxidized form (**Figure 7** and **Table 6**). Each experiment was monitored at 450 nm over the course of reaction completion. For the half-reaction involving 6OHN, the data was fit to a sum of two exponentials.

Wild type had the largest k_{obs1} and k_{obs2} values, serving as a benchmark for the mutations. Similar to the oxygen electrode results, the lysine to methionine mutation had the greatest impact on the reductive half reaction, with the lowest observed rate constants. Looking at the k_{obs1} and k_{obs2} values, both are about 100-fold smaller than wild type. This demonstrates the significance of the lysine residue in the active site of 6HLNO towards reacting with 6OHN. The E292T mutation produced similar results as observed in the steady-state assays where enzyme activity had the second largest impact out of the mutations made, with a 100-fold decrease in k_{obs1} and a 10-fold decrease in k_{obs2} as compared to wild type. These results demonstrate that the glutamate at position 292 also plays a significant role in the reactivity of the enzyme with 6OHN.

Interestingly, the double mutant was only marginally impaired with the reductive half reaction relative to the wild type, a similar observation seen in the steady-state assays. The first and second k_{obs} values are both 10-fold lower than wild type. This is observed with both reaction rate constants for the reaction.

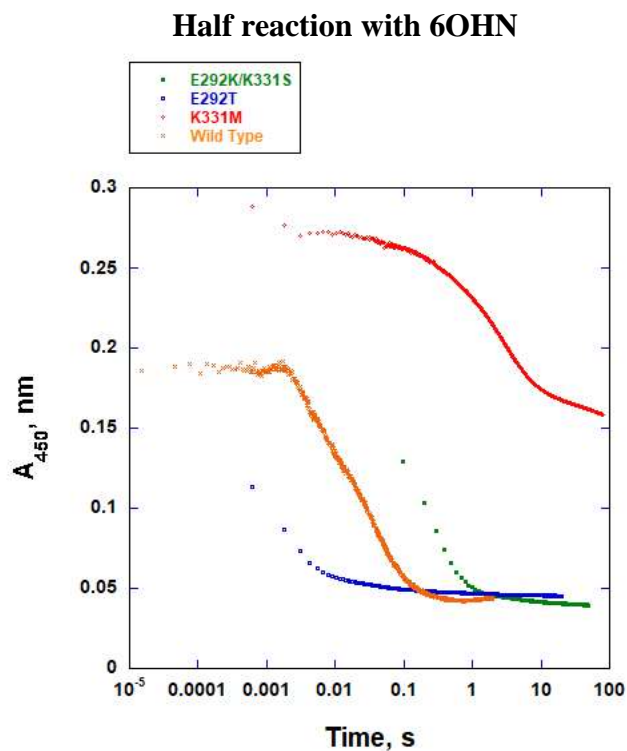


Figure 6: A kinetic trace of the half reaction of 6HLNO-SE with 6OHN at an absorbance of 450 nm. This figure contains a kinetic trace for each mutant as well as wild type 6HLNO-SE. The data is plotted on a logarithmic time axis.

Rate constants for reaction of 6HLNO-SE with 6OHN

	k_{obs1}	k_{obs2}
Wild Type	132.21	19.762
K331M	4.8584	0.36163
E292T	6.6836	0.57014
E292K + K331S	3.1257	0.12419

Table 5: The rate constants calculated for wild type and mutant 6HLNO-SE reacting with 6OHN at an absorbance of 450 nm. The units are absorbance units per second, nm s^{-1} .

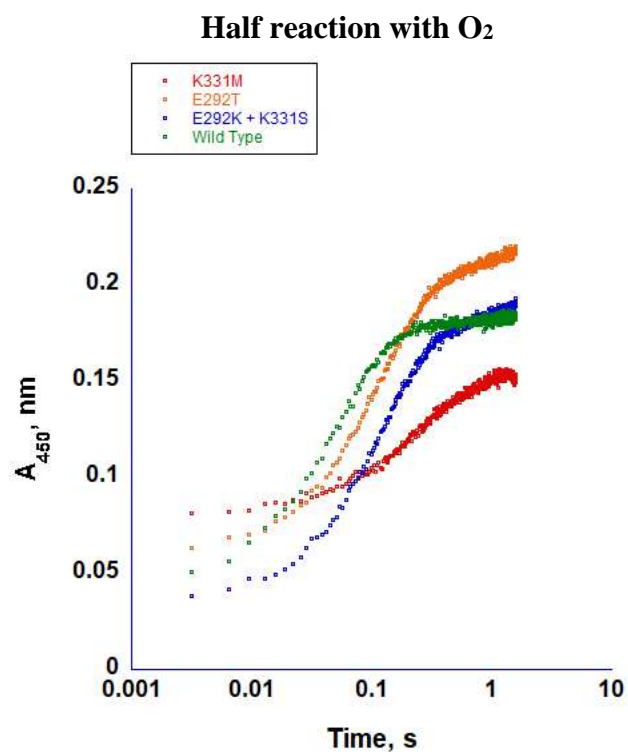


Figure 7: A kinetic trace of the half reaction of 6HLNO-SE with molecular oxygen. As in Figure 4 above, this figure contains a kinetic trace for each mutant as well as wild type 6HLNO-SE. The data is plotted on a logarithmic time axis.

Rate constants for reaction of 6HLNO-SE with O₂

	<i>k_{obs}</i>
Wild type	18.034
K331M	0.013933
E292T	0.27891
E292K + K331S	0.70191

Table 6: The rate constants calculated for wild type and mutant 6HLNO-SE reacting with molecular oxygen at an absorbance of 450 nm. The units are absorbance units per second, s⁻¹.

Similar results as the half-reaction with 6OHN are observed for the half-reaction with O₂. The same pattern that has been observed with the steady state assays is shown to carry through with the transient state assays. Most notably, the lysine to methionine mutation at position 331 has the greatest impact on the reaction of the reduced enzyme with O₂ (about a 1000-fold decrease in *k_{obs}* value), an observation that carries throughout each assay. It can be seen as well that E292T continues to have the second largest impact throughout each assay performed, with about a 100-fold decrease in the observed rate constant when compared to wild type. It had been previously observed that the double mutant resulted in considerable reactivity in both the steady-state oxygen electrode reaction and the transient-state half reaction with O₂. However, here it is observed that it has a 100-fold decrease in activity when compared to wild type. All mutants demonstrate a rate limiting reaction with O₂.

Discussion

The steady-state assays for both mutagenesis and pH-dependence in combination with the transient assays were able to provide evidence that *Shinella* and *Arthrobacter* 6HLNO enzymes behave similarly, despite being distantly related. Steady-state assays were conducted via an O₂ electrode which measured oxygen consumption over time. Similar assays had previously been explored with *Arthrobacter* 6HLNO in which the lysine residue at position 287 was of utmost interest. These assays were able to conclude that the lysine residue is critical for the enzymatic activity in catalyzing the oxidation of (S)-6-hydroxynicotine to 6-hydroxypseudooxynicotine⁴. In 6HLNO-SE, the critical lysine residue was determined to be the one at position 331, which is not homologous to position 287 in *Arthrobacter* 6HLNO. By mutagenesis and steady-state assays, it was demonstrated that this lysine is indeed critical for activity, just as seen in the *Arthrobacter* 6HLNO. This result is observed in every assay performed throughout the study. Other mutagenesis results were able to demonstrate the important role of glutamate at position 292. K331 and E292 are in close proximity in the active site, both pointing toward the flavin. By mutating the glutamate to a threonine, the interaction between residues was disrupted and enzyme activity significantly impacted. By including residues that are present in NicA2 but not *Shinella* 6HLNO, the double mutation, E292K + K331S, was an attempt to make the *Shinella* active site like that of NicA2. The steady-state assays demonstrated that the enzyme was not nearly as efficient as wild type, but still had a k_{cat} value higher than that of the other mutations. This led to further inquiry by use of transient assays to further understand this relationship. Overall, the K_M values were not drastically affected by the mutants for the steady-state assays.

The oxygen electrode results were supported by transient assays by use of stopped-flow. The 6-hydroxy-nicotine oxidase and oxygen half-reactions gave results comparable to the ones received by the oxygen electrode. The k_{obs} values followed the same pattern as k_{cat} for steady-state, where the K331M mutation had the largest decrease in enzyme activity, further supporting the hypothesis of the critical nature of the lysine residue in the active site. For both reductive and oxidative half reactions, a decrease in k_{obs} is seen, supporting the idea that the lysine residue is critical for both half reactions, as seen in the *Arthrobacter* enzyme¹. In that particular study, it was shown that the lysine residue has two critical roles: there is a hydrogen bond mediated by the lysine residue and water which is important for proper positioning of the flavin with its substrates and the positive charge acts as a proton donor when the flavin is undergoing oxidation⁴. Since similar results are seen with 6HLNO-SE, it can be concluded that the same is true of the shifted lysine residue in this study. The E292K mutation also demonstrated a significant impact to enzyme activity, however, not as great as the lysine mutation. These results show the significance of the glutamate residue in the active site in its relation and reactivity with the lysine residue. The double mutant demonstrated similar results as seen in the steady-state k_{cat} values, where enzyme activity was neither fully disrupted nor fully restored. In doing so, the results from the stopped-flow experiments demonstrate that what was observed in the steady-state oxygen electrode assay is observed in both half-reactions, where enzyme activity is improved compared to the K331M mutant, although not significantly. However, the half reaction with molecular oxygen demonstrated a drastic decrease in reactivity for each mutant, signifying a limiting step in the overall mechanism.

The pH-dependence results are comparable between *Shinella* and *Arthrobacter*. Both profiles give a bell curve from which the pK_a values can be determined for the active site. In

terms of pK_a values themselves, they are also comparable between the two enzymes. The larger difference in basic pK_a values is attributed to the different location of the lysine residue in 6HLNO-SE as compared to evolutionary history. This shift could be causing a different electrostatic environment, therefore causing the observable shift in pK_a value. While this is the case, the results suggest similar overall reactivity based on the bell-shape profile and comparable acidic pK_a values, which has been attributed to the enzyme-bound substrate state in the active site of the enzyme and the different states of protonation it can observe.

Thus, the overall reactivity, although not exact, is largely similar between these two enzymes. Though having a distant relation, they have evolved to perform the same function and have similar mechanisms by which they do so. They belong to the same monoamine oxidase structural family of enzymes because of their possession of the conserved FAD and similar reactivity. Most notably, it is observed that the lysine residue in this MAO structural family is critical for reactivity of the enzymes that belong to it, as supported by the similar reactivity between *Shinella* and *Arthrobacter* 6HLNO enzymes.

References

- (1) Office of the Surgeon General; U S Department of Health Human Services. *E-Cigarette Use among Youth and Young Adults: A Report of the Surgeon General*; Createspace Independent Publishing Platform: North Charleston, SC, **2017**.
- (2) Mishra, A.; Chaturvedi, P.; Datta, S.; Sinukumar, S.; Joshi, P.; Garg, A. Harmful Effects of Nicotine. *Indian J. Med. Paediatr. Oncol.* **2015**, *36* (1), 24–31. <https://doi.org/10.4103/0971-5851.151771>.
- (3) *Tobacco and its environmental impact: an overview*. Who.int. <https://apps.who.int/iris/bitstream/handle/10665/255574/9789241512497-eng.pdf> (accessed 2023-03-31).
- (4) Fitzpatrick, P. F.; Chadegani, F.; Zhang, S.; Dougherty, V. Mechanism of Flavoprotein L-6-Hydroxynicotine Oxidase: PH and Solvent Isotope Effects and Identification of Key Active Site Residues. *Biochemistry* **2017**, *56* (6), 869–875. <https://doi.org/10.1021/acs.biochem.6b01160>.
- (5) Dulchavsky, M.; Clark, C. T.; Bardwell, J. C. A.; Stull, F. Author Correction: A Cytochrome c Is the Natural Electron Acceptor for Nicotine Oxidoreductase. *Nat. Chem. Biol.* **2021**, *17* (3), 360. <https://doi.org/10.1038/s41589-021-00756-z>.
- (6) Fitzpatrick, P. F.; Chadegani, F.; Zhang, S.; Roberts, K. M.; Hinck, C. S. Mechanism of the Flavoprotein L-Hydroxynicotine Oxidase: Kinetic Mechanism, Substrate Specificity, Reaction Product, and Roles of Active-Site Residues. *Biochemistry* **2016**, *55* (4), 697–703. <https://doi.org/10.1021/acs.biochem.5b01325>.
- (7) Choudhary, V.; Wu, K.; Zhang, Z.; Dulchavsky, M.; Barkman, T.; Bardwell, J. C. A.; Stull, F. The Enzyme Pseudooxynicotine Amine Oxidase from *Pseudomonas Putida* S16 Is Not an Oxidase, but a Dehydrogenase. *J. Biol. Chem.* **2022**, *298* (8), 102251. <https://doi.org/10.1016/j.jbc.2022.102251>.
- (8) Moran, G. R. Anaerobic Methods for the Transient-State Study of Flavoproteins: The Use of Specialized Glassware to Define the Concentration of Dioxygen. *Methods Enzymol.* **2019**, *620*, 27–49. <https://doi.org/10.1016/bs.mie.2019.03.005>.

Contributions & Acknowledgements

I want to thank the outstanding support and mentorship I have received in the Stull lab and its members. I also want to thank Dr. Stull and his incredible guidance and help in this project as well as Dr. Barkman and his support being a member of my committee. I also received funding for this project, which is listed below.

Undergraduate Award for Research & Creative Excellence Scholarship – Fall 2022

Lee Honors College Research & Creative Activities Scholarship – Spring 2022